Multidisciplinary analysis and design of strut-braced wing concept for medium range aircraft

Gérald Carrier, Guillaume Arnoult, Nicolo Fabbiane, Jean-Sébastien Schotté, Christophe David, Sébastien Defoort, Martin Delavenne, Emmanuel Bénard

Multidisciplinary analysis and design of strut-braced wing concept for medium range aircraft

Gérald Carrier[1], Guillaume Arnoult[2], Nicolo Fabbiane[3], Jean-Sébastien Schotté[4],
ONERA, Paris Saclay University, F-91123, Palaiseau, France
Christophe David [5], Sébastien Defoort[6]
ONERA, Toulouse University, F-31055 CEDEX 4, Toulouse, France
Martin Delavenne [7], Emmanuel Bénard[8]
ISAE-SUPAERO, Université de Toulouse, F-31055 Toulouse, France

Increasing the wing aspect ratio appears as a straightforward way to improve aerodynamic performance of transport aircraft by reducing the lift-induced drag component. However, it comes at the price of a direct negative impact on the wing structural weight which is necessary to sustain aerodynamic loads in the case of a conventional cantilever wing. The strut-braced wing concept allows to reduce the flexural moment to be carried out by the inner-wing structure and therefore limits the weight penalty as aspect ratio is increased. A multidisciplinary evaluation of the potential benefits at aircraft level of High Aspect Ratio, Strut Braced Wing concept is presented. It relies on a multi-fidelity design approach in which an Overall Aircraft Conceptual Design framework is combined with high-fidelity aerodynamic and structural analyses to provide accurate physical information to the conceptual design process. This paper describes the tools, framework and approach used to combine OACD with high-fidelity CFD and CSM analyses and illustrates the first results of its application to design a HAR-SBW aircraft concept which are compared to a conventional tube-and-wing aircraft designed for the same mission.

---

[1] Research Engineer, Aerodynamics, Aeroelasticity and Acoustics Department, AIAA Member.

[2] Research Engineer, Aerodynamics, Aeroelasticity and Acoustics Department.

[3] Research Engineer, Aerodynamics, Aeroelasticity and Acoustics Department.

[4] Research Engineer, Aerodynamics, Aeroelasticity and Acoustics Department.

[5] Research Engineer, Information processing and Systems Department.

[6] Research Engineer, Information processing and Systems Department.

[7] Research Engineer, ISAE-SUPAERO-DCAS Department.

[8] Ass. Prof., ISAE-SUPAERO-DCAS Department.

I. Nomenclature

AR = Aspect Ratio

BWB = Blended Wing Body

HAR = High Aspect Ratio

CFD = Computational Fluid Dynamics

LR = Long Range

CSM = Computational Structural Mechanics

OACD = Overall Aircraft Conceptual Design

SBW = Strut Braced Wing

SMR = Short Medium Range

VLM = Vortex Lattice Method

II.Introduction

Reducing the environmental footprint of aviation and especially its impact on climate change has now become the major challenge of the aeronautical industry. In this context, the European Commission has set ambitious goals for aviation defined in the "Fligthpath 2050"[1], including 75% reduction of CO2 and 90% reduction of NOx emissions, as well as a 65% reduction of noise. Achieving such targets will likely be possible only through radical evolutions of the aircraft architecture, propulsion system and the introduction of disruptive technologies. For what concerns the aircraft architecture, the Blended Wing Body (BWB) and the Strut-Braced Wing (SBW) seem today to be the two most promising alternatives to the conventional "Twin Underwing Turbofan Tube-and-Wing" configuration that has become the predominant solution over the last decades. The BWB, and the Hybrid Wing Body, are currently investigated in several important research efforts in Europe, USA and China [2][3][4]. The present paper addresses investigations of the SBW configuration. The main rationale for the SBW configuration is to enable significant increase of the wing aspect ratio (AR) to improve overall aircraft performances through aerodynamic efficiency gains without the tremendous wing weight increase that a cantilever wing of similar AR would suffer from. This is achieved through a reduction of the bending moment in the inner wingbox permitted by a traction of the strut at its junction with the wing, as illustrated in Figure 1. This enables to downsize the wing box structural components in the inner wing that are primarily sized by the bending moment in the case of a cantilever wing.

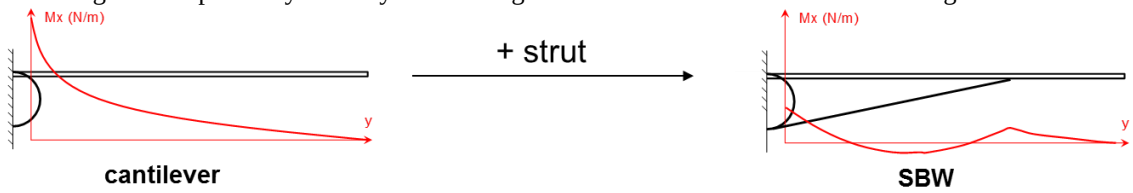

Figure 1 - Reduction of inner wing flexural moment by the SBW concept.

This concept can be used to increase the wing aspect ratio and take advantage of an aerodynamic efficiency improvement obtained by reducing the lift induced drag component, while alleviating the increase of the wing structural weight associated with higher span (involving higher bending moment in the central wing-box). Therefore adding a strut, or more generally a truss structure, opens an additional degree of freedom for the designer to better exploit high aspect ratio wings at overall aircraft level by achieving new and better trade-off between aerodynamic efficiency and wing weight, compared to conventional cantilevered-wing concept.

Such trade-offs for the SBW were already investigated at ONERA in the ALBATROS project [5]. More recently, in the Clean-Sky 2 thematic topics project U-HARWARD [6] different aircraft-level solutions enabling wing aspect ratio increase (such as cantilever flexible wings, SBW and folding wingtips) are currently investigated to reduce the environmental impact and improve the overall aircraft performance. In this project, ONERA and ISAE-SUPAERO

are exploring the potential benefits and eventual pitfalls of the HAR-SBW concept through a multi-level multi-disciplinary design approach including overall aircraft conceptual design (OACD) and refined disciplinary design studies of the aerodynamic and structural key aspects of HAR-SBW concept by high fidelity analysis methods.

This paper describes the investigation of the HAR-SBW concept and tries to evaluate its potential benefits at overall aircraft level. Basically, our objective is to explore the impacts at aircraft level of the increase of the wing aspect ratio, with and without strut and identify what are the maximum benefits expectable with and without strut and for which values of AR (and wing design parameters) this occurs.

The conceptual design approach used to assess the overall aircraft impacts of HARW and SBW concepts is introduced in the first section. Then the high fidelity aerodynamic analysis and design approach developed and used for this project to evaluate the HAR-SBW aerodynamic benefits is described and illustrated with preliminary design results in the second section. The third section describes the development of a wing structural weight evaluation module for the SBW concept and illustrates its capabilities. Finally, the last section describes the first results obtained with this multilevel OAD process combining the different models describes in sections 1 to 3 for the HAR-SBW concept. The benefits at overall aircraft level of the SBW concept is evaluated by investigating different values of the wing aspect ratio ranging from 12 to 22 and comparing the resulting aircraft characteristics to those of a conventional tube-and-wing aircraft configuration designed for the same mission with the same tools and approach.

III.Conceptual design approach

A. Top Level Aircraft Requirements (TLAR)

The aircraft investigated are designed for the following mission characteristics, close to the Airbus A321-LR aircraft TLAR:

- a sizing range of 7400 km,
- a sizing payload of 18 tons (~200 pax),
- a maximum payload of 23 tons
- a cruise Mach number of 0.78;

This choice was found to be a good compromise between aircraft size (that could enable to derive conclusions for SMR and even regional mission) and scalability up to longer ranges, where the induced drag savings should provide the best positive effect.

Additionally to above requirements, engines are fixed with a Maximum TakeOff thrust of 134kN.

B. FAST-OAD tools for conceptual design

The ONERA-ISAE *FAST-OAD* aircraft conceptual design framework [7] is used in this work to perform the overall aircraft design in order to maximize the SBW benefits in terms of overall aircraft performances. FAST-OAD is implementing a multidisciplinary sizing process of the aircraft (see Figure 2) and is designed so that models can be added or removed from the process, which allows to adapt the OAD problem to the studied configuration and introduce various fidelity models for the same discipline. First this framework has been applied to generate a conventional aircraft (tube and wing) that meets the chosen TLARs, with the intent of providing a reference configuration to be compared to the SBW designs that will be lately investigated.

The models initially in place in this process (before introducing specific models for the SBW configuration) lie in the family of the so-called “Level 0” (statistical/analytical) models, well adapted for rapid sizing of conventional configurations:

- Geometry: semi-empirical formulas for adapting general characteristics of aircraft to TLARs
- Weight: semi-empirical formulas for estimating weights (detailed breakdown by components)
- Handling Qualities: analytical formulas for sizing empennage and setting wing position along fuselage
- Aerodynamics: analytical and empirical formulas (Oswald coefficient, flat plate friction drag)
- Performances: estimation of fuel consumption using time-step integration of point-mass mission simulations
- Propulsion: semi-empirical parametric model for turbofan engine (directly used by performance model).

The design process of FAST-OAD with this collection of models is validated against an A320-CEO-like configuration [8] (Table 1) and can easily be extended to the parameters of an A321-like aircraft.

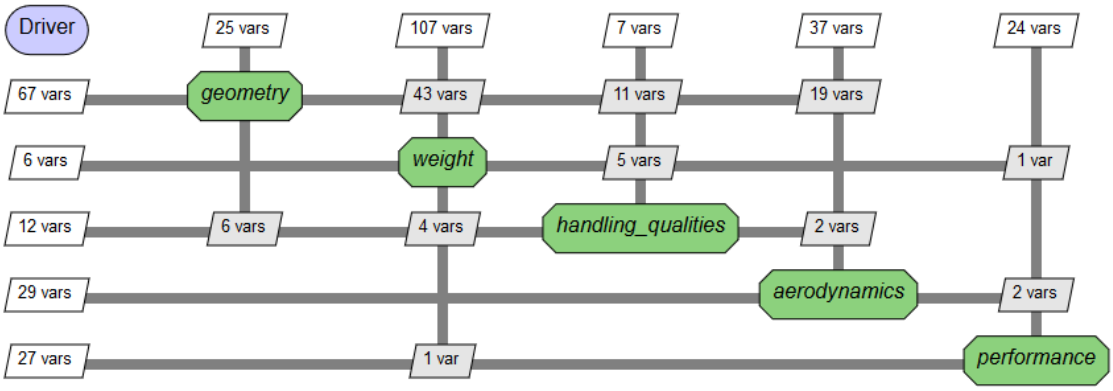

Figure 2- FAST-OAD process (XDSM)

Weight	units	FAST-OAD value	Targeted value	Delta (%)
OWE	kg	42000	42100	-0.24%
MZFW	kg	61608	62100	-0.79%
MFW	kg	18474	18700	-1.21%
MLW	kg	65305	64500	1.25%
MTOW	kg	77006	77000	0.01%
fuel for SPP design mission	kg	19014	18678	1.80%
TOW for SPP design mission	kg	74260	74102	0.21%
fuel for SPP study mission	kg	6281	6665	-5.76%
TOW for SPP study mission	kg	61527	62089	-0.91%

Table 1- Weights from FAST-OAS sizing for CSR-01

The next steps is to introduce in this OAD process the capability to perform a sizing loop on a SBW configuration. Low-fidelity aerodynamic and structural weight evaluation models, specific to SBW, are integrated into the FAST-OAD framework.

1. *Weight/Structure*

The wings and struts primary structure weights are computed using physical analytical models based on beam theory [8]. The wing structure is simplified to an equivalent spar plus skin model with the spar flanges supporting bending moment, the web supporting the shear and the skin supporting the torsion

This methodology has been extended to the SBW considering they only support traction and compression forces, as it will be described in section V. This method requires aerodynamic forces and moment spanwise distributions that can be estimated from elliptical loading or retrieved from Vortex Lattice Method computations as explained below.

Also implemented in FAST-OAD, a beam-like finite element model of the struts and the wings can be substituted to the previous models to compute both primary structural weights and deformations. Sections properties (area and inertia) are computed considering web thickness, equivalent upper and lower skin thickness and stringers area. The weight simply derives from material properties and thickness necessary to sustain static manoeuvre loads (2.5g, -1g).

This approach can be coupled to aerodynamic force computation to size the wings and the struts within an aerostructural process. This approach is relevant for high-aspect ratio wings with non-negligible deformations.

The weight of the other components (fuselage, tails, systems, …) is assessed through statistical formulations.

2. Aerodynamics

Originally, aerodynamic models implemented in FAST-OAD rely on analytical and empirical formulations. The friction drag comes from a flat plate approximation corrected by compressible, sweep, camber and thickness effects. The induced and wave drag are derived from empirical formulations of the Oswald coefficient and critical Mach number estimates. These formulations may be extended to the struts that are mainly accounted through their contribution to viscous drag and their interference with the wing.

Vortex Lattice Method computations can also be performed within FAST-OAD using AVL software [10]. Particularly, loads distributions can be extracted to feed wings and struts weight computations and the aerostructural process.

3. Propulsion

This module, not specific to SBW configuration, is however tweaked with respect to the original turbofan model of the FAST-OAD distribution to mimic the performances of an EIS 2015 engine such as the LEAP-1A, because a future SBW aircraft will likely use that family of turbofans and has to be compared to a –NEO aircraft. Around 10% SFC savings compared to CEO can be expected from this new propulsion model.

IV.High-fidelity Aerodynamic Design and Analysis

A. Description of the parametric automated aerodynamic analysis and design framework

For the sake of performing the aerodynamic design of the SBW configuration and feed the aerodynamic model used in the OAD environment with high-fidelity aerodynamic data , the following Hi-Fi design framework has been set up (Figure 3). First, a fully parametric geometry model has been generated using the Engineering Sketch Pad (ESP)[11] tool developed by MIT. This freely available and open source software allows the user to build its own geometry with different levels of fidelity. This geometry can be connected to Analysis Interface Modules (AIM) through the Computational Aircraft Prototype Synthesis (CAPS)[13] software (for meshing, structural analysis,..). In the current framework, four AIM modules are used and assembled into an automated design analysis chain using plain Python scripts (Figure 3): Pointwise (meshing), SU2 (CFD calculations), Friction module.

The commercial mesh generation software Pointwise enables the engineer to create structured and unstructured meshes, covering a wide range of CFD calculation needs. It is used there in batch mode using the Glyph scripts capability that enables to automate the generation of unstructured CFD mesh around almost arbitrary aircraft geometries [16]. Then, the open-source CFD software SU^2 [21] written in C++ for the numerical solution of partial differential equations, provides the flow field around a geometry and thus, the aerodynamic coefficients (solving either the RANS or Euler equations). Finally, the ONERA Far-Field Drag post-processor FFD00 [14] is used to evaluate lift-induced, wave and viscous drag components and suppress the spurious irreversible drag inherent to numerical CFD solutions.

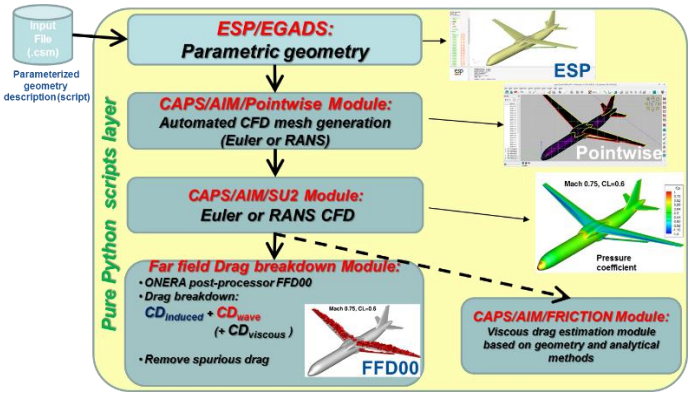

Figure 3 - Aerodynamic design framework based on CAPS/ESP/EGADS tools

B. Aerodynamic analysis and design process set-up and demonstration on A321 aircraft configuration

As introduced in section III.A, the reference configuration considered in this work is a long-range (LR) version derived from a single-aisle (SA) short-to-medium range (SMR) aircraft similar to a A321-LR. Each geometrical parameter is written in the ESP/EGADS and describe in Figure 4 to Figure 6.

Figure 4 - Geometrical parameters associated to the fuselage

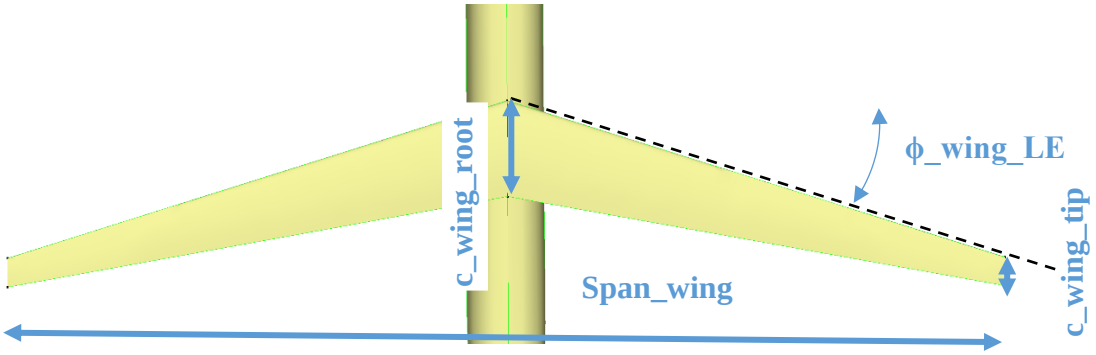

Figure 5 - Geometrical parameters associated to the wing

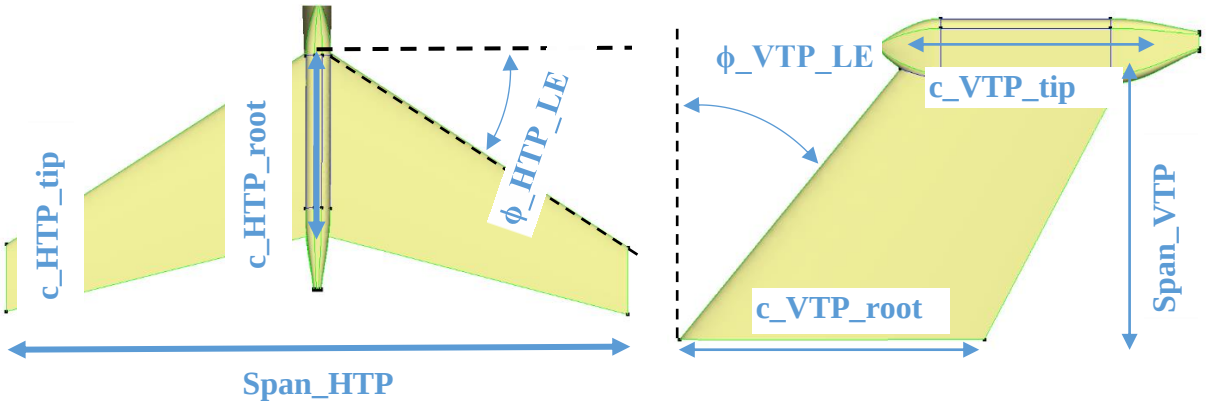

Figure 6 - Geometrical parameters associated to the HTP and VTP

From these parameters, the reference aircraft was modeled according to the values gathered in Table 1.

Parameter	Units	Value
Fuselage Length	m	44.51
Fuselage Width	m	3.95
Fuselage Height	m	4.05
Wing Span	m	34.1
Wing Area	m²	126
Wing Aspect Ratio	-	9.23
Wing Taper Ratio	-	0.25
HTP Span	m	12.45
HTP Area	m²	30.75
HTP Aspect Ratio	-	5.04
HTP Taper Ratio	-	0.37
VTP Span	m	5.87
VTP Area	m²	22.3
VTP Aspect Ratio	-	1.55
VTP Taper Ratio	-	0.26

Table 1 – A321-LR reference aircraft geometrical characteristics used for the reconstruction

An illustration of the reconstructed A321-LR is presented in Figure 7 and used in the process presented in the previous section to achieve CFD simulations and analysis. These computations are performed using SU² solver with target lift coefficients which allows drawing the polar curve of the aircraft.

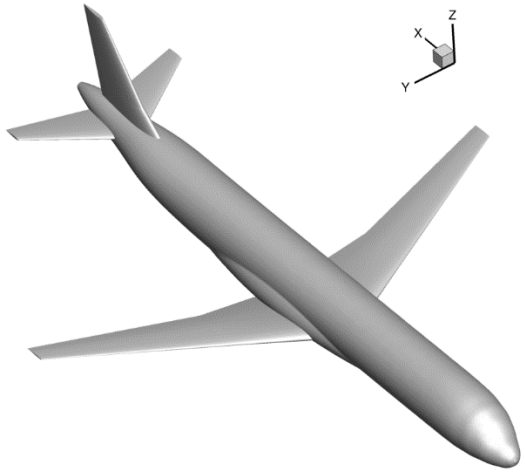

Figure 7 - Reference aircraft geometry

CFD simulations based on both Euler and RANS (Reynolds Averaged Navier-Stokes) modelling are achieved on this configuration for several Mach numbers. The analysis can be performed either in the near field, for instance as illustrated in Figure 8 with the surface pressure coefficients

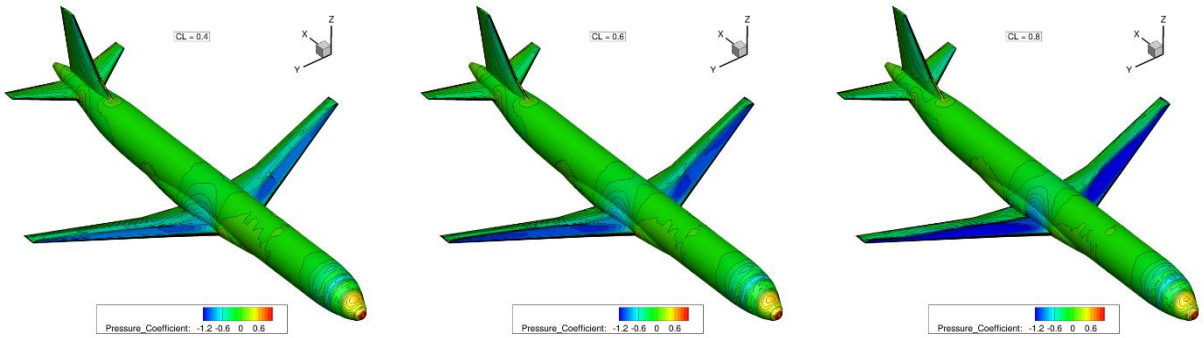

Figure 8 - Pressure coefficient distribution on the reference aircraft at M = 0.78, RANS (Spalart-Allmaras) modelling of the flow

A far field analysis is also performed during the process to identify the drag components, as shown in Figure 9 where the influence of the Mach number on the viscous (triangle shape), wave (diamond shape) and induced (circle shape) components of the drag is illustrated.

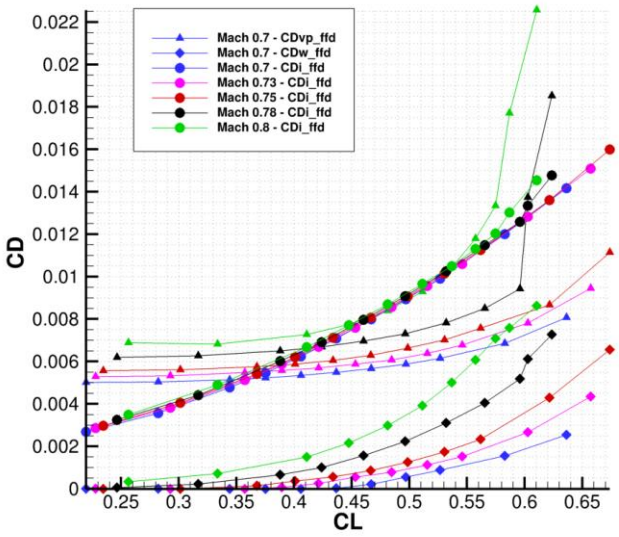

Figure 9 - Influence of the Mach number on the drag decomposition for the reference aircraft, CFD computations achieved with RANS modelling of the flow

These results are considered as the starting point of the present study to conclude on the effect of the strut on the configuration performances.

C. Aerodynamic analysis and design of the SBW aircraft configuration

1. SBW aircraft geometry parameterization

The objective of this part of the study is to define a generic parameterization of the strut, which will be used in the future for optimization purposes. The geometry of the strut is thus defined by 9 top-level parameters, which are gathered in Table 2.

Parameter	Units	Description
Span_frac	-	Fraction of the wing span
Strut_emp_Z	m	Position in the Z-direction of the junction between the strut and the fuselage
Strut_emp_Y	m	Position in the spanwise-direction of the junction between the strut and the fuselage
Strut_curvature_radius	m	Radius joining the “vertical” and “horizontal” components of the strut
Strut_Vert_sweep	°	Sweep angle of the “vertical” part of the strut
Strut_LE_sweep	°	Sweep angle of the “horizontal” part of the strut
Junction_TR	-	Ratio applied to the wing chord at the junction between the strut and the wing
Strut_Vert_twist	°	Twist angle of the “vertical” part of the strut
Strut_twist	°	Twist angle of the “horizontal” part of the strut

Table 2 – SBW geometry parameters describing the strut

These last parameters are directly taken from an aerodynamics consideration since they are supposed to have an influence on the channel effect described in [5] and induced by the junction between the wing and the strut, leading to an important contribution of the wave drag to the global drag of the aircraft.

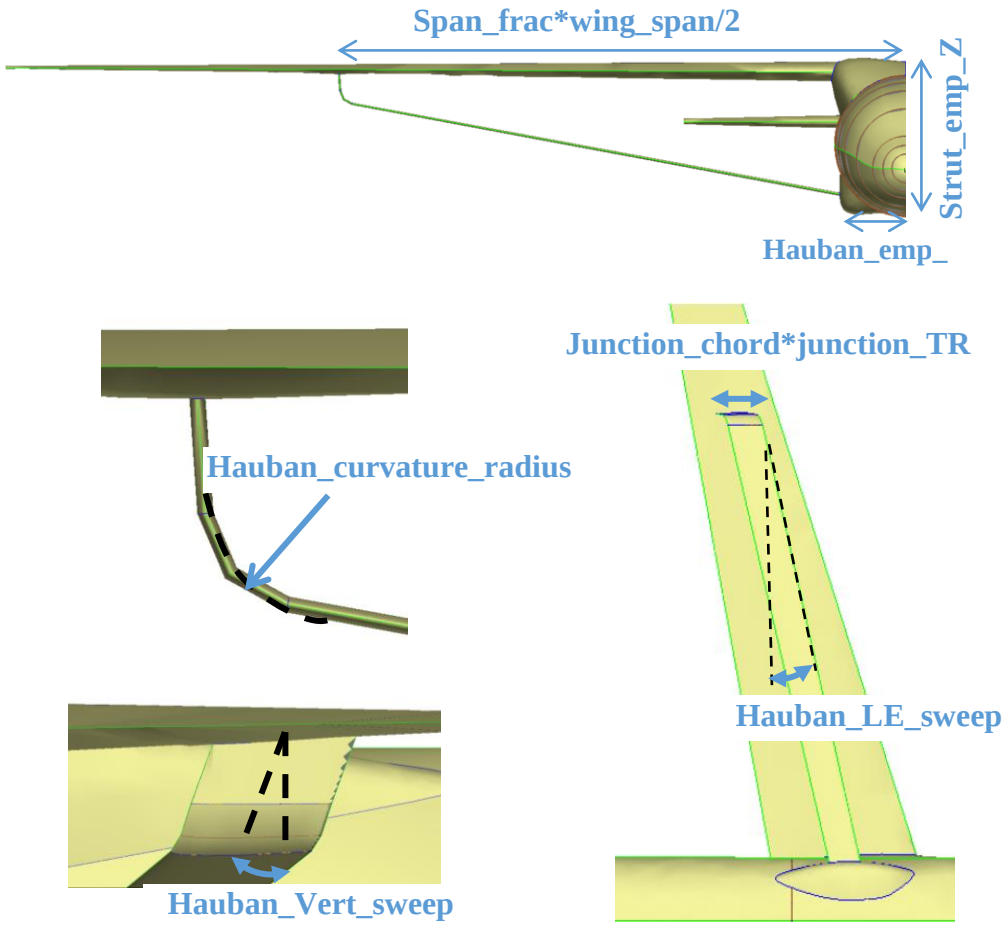

Figure 10 - Illustration of the geometrical parameters associated to the strut

2. Aerodynamic analysis of the reference Strut-Braced Wing configuration

The reference configuration for this part of the study is taken from a former project studied at ONERA, called ALBATROS and described in [5]. This specific configuration, illustrated in Figure 11, is reconstructed using the ESP/EGADS tools in the same way as the A321-LR reference configuration for the cantilever wing.

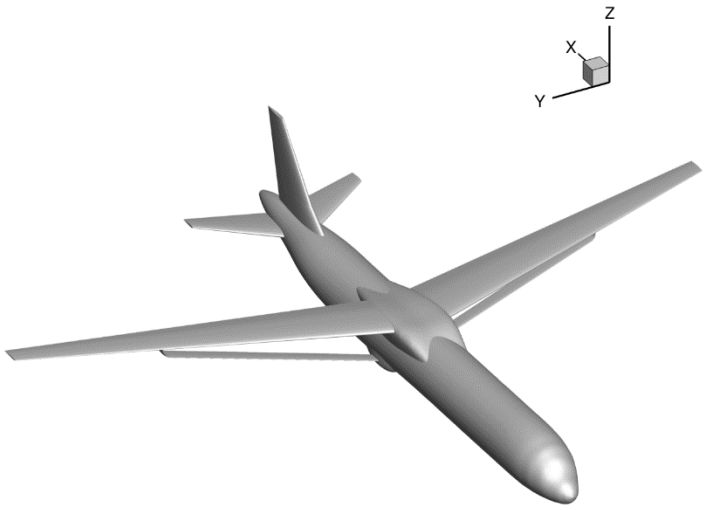

Figure 11 - Reconstruction of the ONERA ALBATROS configuration using ESP/EGADS tools

CFD computations are achieved at cruise conditions of the mission defined earlier using Euler flow modelling at a Mach number M = 0.78 and for several target lift coefficients. The Far Field Drag post-processing included in the process allows identifying the sources of the different drag components, as illustrated in Figure 12 for the wave drag.

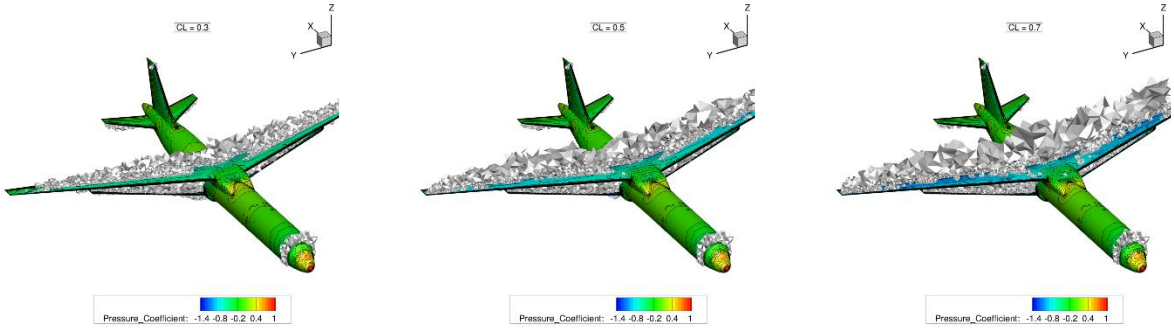

Figure 12 - Wave drag sources based on Euler simulations on the reference Strut-Braced Wing configuration

After these first computations, it appears that the conventional tail configuration is not well adapted for this kind of configurations. The engines could be located either under the wing (which induces high interaction with the strut) or at the rear of the fuselage. In both cases, the engine exhaust would impact directly the HTP, with the risk of reducing its efficiency. A T-Tail configuration is thus designed and used in the next steps of the study, as illustrated in Figure 13.

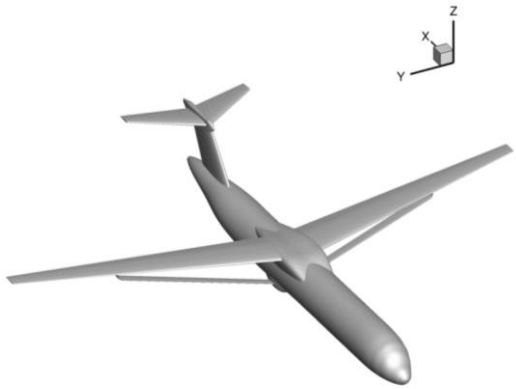

Figure 13 - Modelling of the T-tail geometry

3. Construction of a strut analytical modelling

Based on this last geometrical modelling, the influence of the strut on the drag components is studied. To perform this analysis, a strut-less aircraft configuration and a rear strut-braced configuration are considered. Both configurations are illustrated in Figure 14. The aim here is to isolate the contribution of the strut to define an analytical model of the additional drag generated by the strut that could be integrated in the FAST-OAD process. RANS meshes are automatically generated (Figure 14) with Pointwise and SU² computations are achieved for the target lift coefficients in [0.3; 0.4; 0.5; 0.6; 0.7; 0.8].

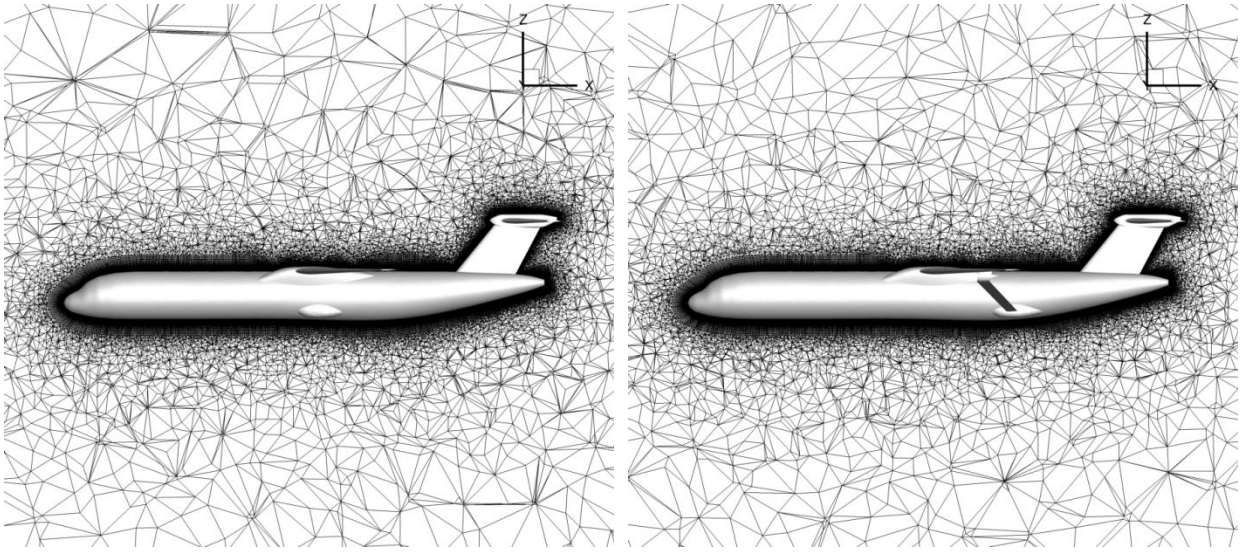

Figure 14 - Illustration of strut-less and rear strut-braced configurations

The rear strut-braced configuration is considered here as it allows reducing the interaction between the wing and the strut, thus lowering the impact of the channel effect and the wave drag generated by the configuration.

In order to generalize this modelling to any strut geometry that will be considered in the future, only the additional friction drag is considered here and multiplied by the ratio $\frac{Swet_{wing}}{Swet_{strut}}$. The evolution of this coefficient is shown in Figure 15 as a function of the lift coefficient at which the computations were achieved.

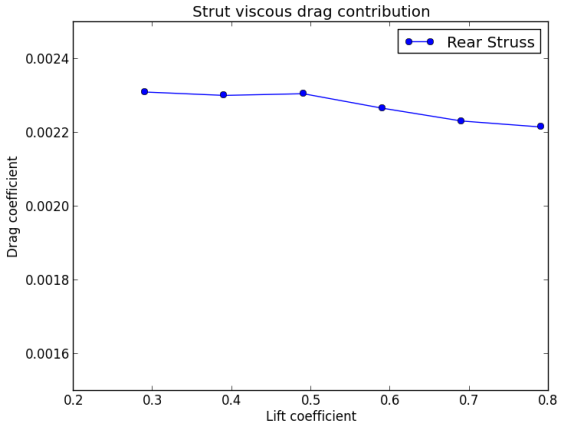

Figure 15 - Strut viscous correction factor

This is then directly usable in the FAST-OAD framework to rapidly evaluate the viscous drag induced by a strut and identify the most promising design of strut-braced wing configurations from the aero-structural point of view resulting in optimum overall aircraft performances.

The sweep values considered here are not optimum but the authors hope to be able to identify an optimum configuration in the future and examine its impact on the other disciplines involved in the design process of the strut-braced wing configuration.

4. Illustration of aerodynamic design optimization capability for the SBW configuration

The CFD-based aerodynamic analysis process described previously (Figure 3) can be used to perform automated aerodynamic design optimization by linking this parametric analysis process with a numerical optimization algorithm. The capability of conducting aerodynamic design based on shape optimization using the present set of tools is illustrated hereafter. For that a simplified wing design exercise on the SBW configuration is performed using gradient based optimization and Euler flow modelling.

The optimization problem is defined as a full SBW aircraft inviscid drag minimization in transonic cruise condition (Mach number 0.78) at constant lift coefficient (CL=0.5). A subset of the complete set of geometry parameters defined in the ESP model are used to control the airfoil geometry of the wing. Fourteen design parameters are used to control simultaneously the wing twist and the wing airfoil geometry using the implementation of the CST airfoil parameterization by Kulfan[19]. The optimization was performed using the Modified Method of Feasible Direction algorithm of Vanderplaats[20] and included a constraint on the minimum wing airfoil relative thickness of 10%, while the initial wing geometry is equipped with aifoil of 12% relative thickness.

The evolution of the 14 design variables and optimization functions are plotted in Figure 16. A comparison of the initial and optimized airfoil geometry with the corresponding pressure distributions on an outboard wing section at 75% of span is given in Figure 17. The optimization achieved a reduction of the inviscid drag of about 100 drag counts, thanks mostly to the reduction of the wave drag which was significant on the initial configuration due to the “channel flow” between the wing intrados and the strut in these transonic flow conditions as it is illustrated in Figure 18. The wing extrados pressure recovery is also significantly improved as illustrated in Figure 17 and Figure 18.

This demonstrates that the CFD-based parameterized aerodynamic model of the complete configuration can be successfully used to perform basic aerodynamic design tasks by automated optimization. This capability is particularly important for evaluating the aerodynamic efficiency in transonic flow condition of an aircraft concept such as the SBW and deriving aerodynamic data that can be used in an OAD process like in III.B

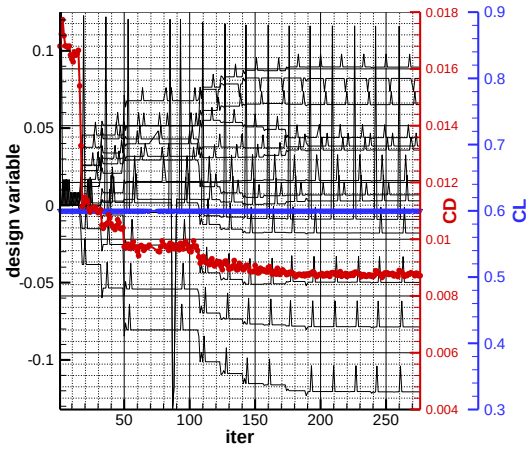

Figure 16 - History of evolution of airfoil geometry variables during the aerodynamic drag minimization by gradient-based optimisation

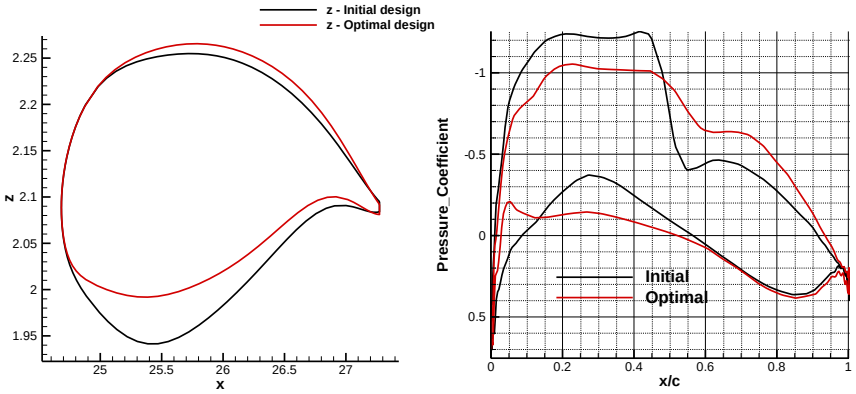

Figure 17 - Comparison of airfoil geometries and pressure distributions on the initial and optimized wing design

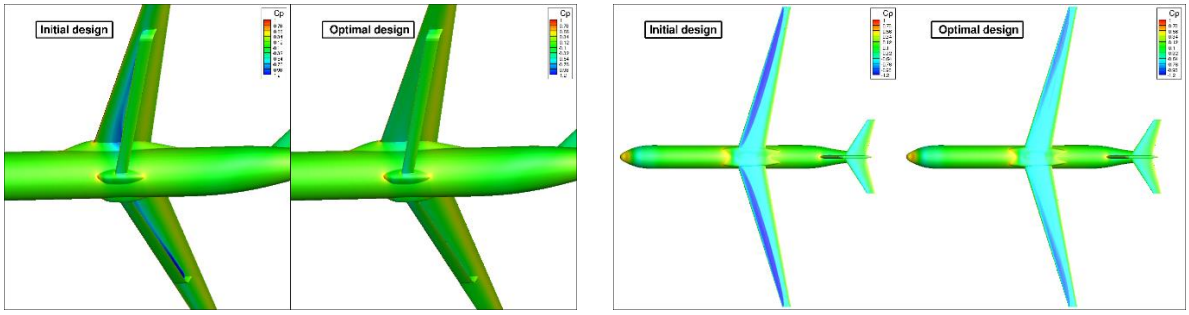

Figure 18 - Comparison of pressure distributions on the initial and optimized wing design

5. Illustration of engine integration design capability

The CFD-based process with parameterized geometry based on ESP [11] was also used successfully to investigate engine integration aspect on the SBW configuration. A geometry model of a generic high by-pass ratio engine nacelle was developed with ESP and added to the glider configuration, hold by a basic (parallel flange) engine

pylon of adaptive length. This enabled straightforward parametric investigation of the impact of engine position and settings (toe and pitch angle) on the overall aircraft aerodynamic coefficients, as it is illustrated in Figure 19. Each of the configurations corresponding to underwing and rear-fuselage mounted engine locations could be analysed by just changing the values defining the position, pitch and toe angles of the nacelle in the geometry model.

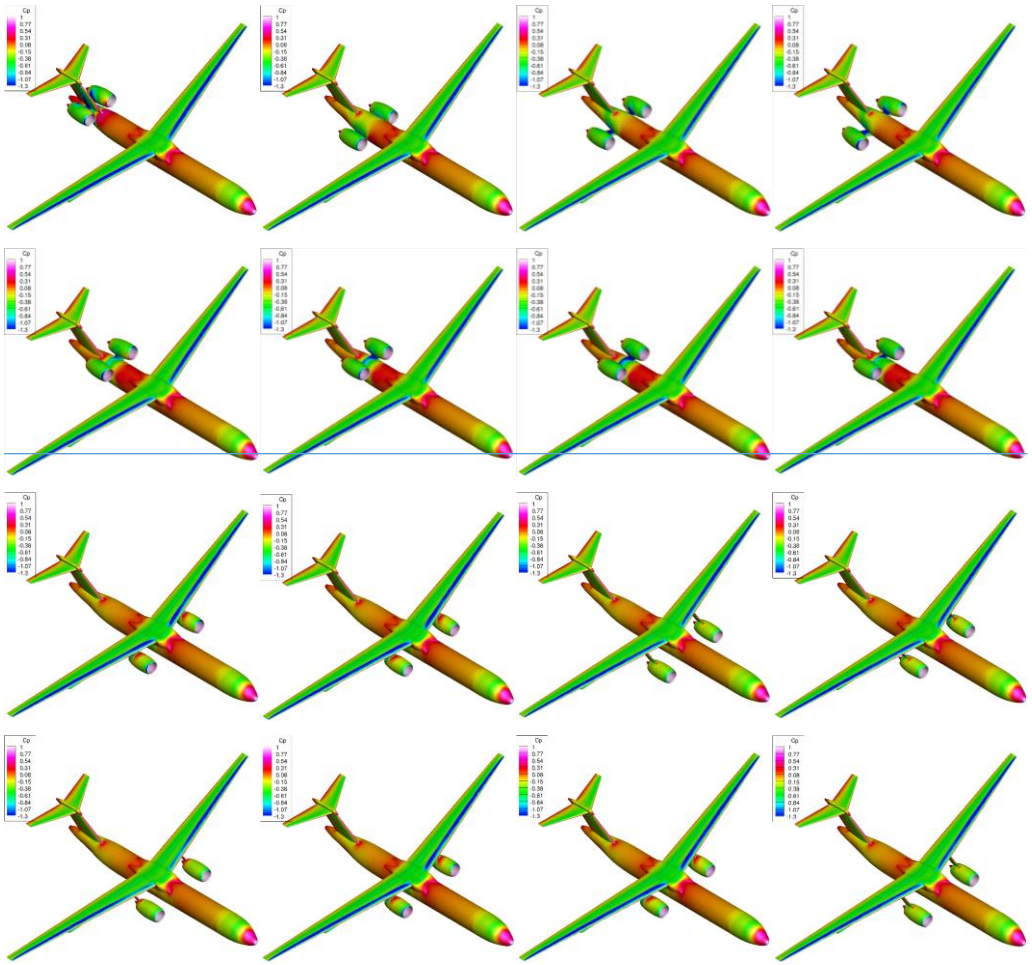

Figure 19 - Illustration of different variants of engine integration investigated with the automated CFD-based analysis process

V. Structural Design and Analysis of the SBW configuration

A. Construction of a wing weight estimation model for the SBW configuration

As exposed above, the initial version of FAST-OAD relies on semi-empirical formulas for weight estimates and aerodynamics. In order to account for strut-braced wing configurations, new loads, weight estimates and aerodynamic models have been integrated within FAST-OAD framework.

1. Wing loads model

First, a loads evaluation module has been set up to compute both limit and ultimate load factor (n_z) considering a safety factor imposed by the user, typically 1.5. So far, only one load case is implemented that consists in a pull-up manoeuvre at MTOW. Then, specific sub-models are developed to compute the external and corresponding internal loads resulting from aerodynamic, fuel distribution, engines, structural weight itself and induced by the strut. Only the aerodynamic loads computation is mandatory, the consideration of other contributions is let to the user.

a. Geometric considerations

Prior to any loads computations, some geometric considerations have to be introduced. As illustrated in Figure 20, parameters are introduced to take into account the geometry of the wing box. Particularly, the local wingbox chord is deduced from the local aerodynamic chord considering the spars chord ratios and a projection factor, f_{ϕ_e}, to account for the ratio between the chord in aerodynamic axis and its projection onto elastic axis:

$$c_{box(y)} = \left(k_{rear-spar} - k_{front-spar}\right) \cdot c_{aero}(y) \cdot f_{\phi_e} \cdot \cos\phi_e$$

The location of the elastic axis, is defined from the contribution of each spar to the inertia of the box. This contribution, x, is fixed by the user and the chord-wise location of the elastic axis is deduced from rear and front spar ratios as follows:

$$k_{ea} = x \cdot k_{front-spar} + (1 - x) \cdot k_{rear-spar}$$

The height of the wingbox is also approximated from airfoil characteristics considering the relative thickness and a coefficient that takes into account the non-rectangular shape of the box, k_{spar}, whose typical value is around 0.93:

$$h_{spar} = k_{spar} \cdot c_{aero} \cdot e_{airfoil}$$

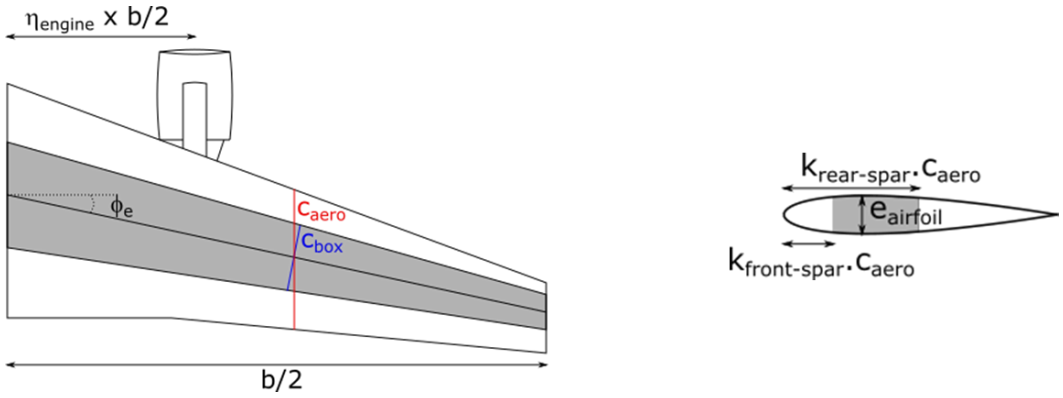

Figure 20 - Wingbox parametrisation for loads computation

This parametrization is valid whatever the wing type considered (cantilever or strut-braced). But, the consideration of the SBW configuration requires additional geometric parameters that have been introduced in section C.1 and are summarized for what concerns the present structural model in Figure 21. Particularly, the strut/wing junction relative location, η_{strut} and the distance between wing and strut roots, h_{strut}, note also that the chord of the strut is assumed to be constant span-wise as well as the size of the box. Figure 21 also shows the selected convention of the internal forces orientation applied for loads computation.

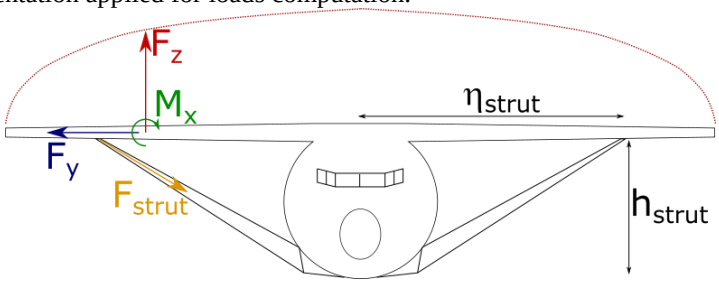

Figure 21- Strut-braced wing parametrization and internal forces orientation.

b. Aerodynamic loads

In the current version of FAST-OAD, no assumption about lift distribution is made. Therefore, a new model capable of estimating the local lift has been developed, either from a simple elliptical loading for rapid evaluations or from a computation with a Vortex Lattice Method taking into account airfoil camber, wing planform and twist.

The aerodynamic shear is then computed at any load section considering the local lift distribution $l(y)$:

$$F_{z,aero}(y_{load}) = \int_{y_{load}}^{b/2} l(y)dy$$

Then, the bending moment is deduced, taking into account the local sweep angle of the elastic axis with respect to aerodynamic reference axis ϕ_e:

$$M_{x,aero}(y_{load}) = \int_{y_{load}}^{\frac{b}{2}} \frac{F_z(y)}{\cos\phi_e} dy$$

The local torque is also considered through two contributions. The first one resulting from the natural pitching moment of the airfoil, the second due to the distance between the aerodynamic centre and the elastic axis. To simplify the computations, the aerodynamic centre is assumed to be located at 25% of the local chords independently of the spanwise location.

$$M_{y,aero}(y_{load}) = \frac{1}{2}\rho V^2 \cos^4\phi_e f_{\phi_e}^4 c_{m,airfoil} \int_{y_{load}}^{\frac{b}{2}} \frac{c_{aero}^2}{\cos\phi_e} dy + (k_{ea} - 0.25)\cos\phi_e \int_{y_{load}}^{\frac{b}{2}} c_{aero} l(y)dy$$

c. Fuel loads

The fuel distribution is also considered for internal loads computation. The wing is divided into three tanks (center, inner, outer) as illustrated in Figure 22. The 20% outermost part of the wing is considered empty. Besides, the filling of each tank can be controlled individually through filling coefficients ($k_{fill,ct}, k_{fill,it}, k_{fill,ot}$) that range from 0.0 to 1.0. The fuel density ρ_{fuel} is set to 0.78kg.m^{-3}.

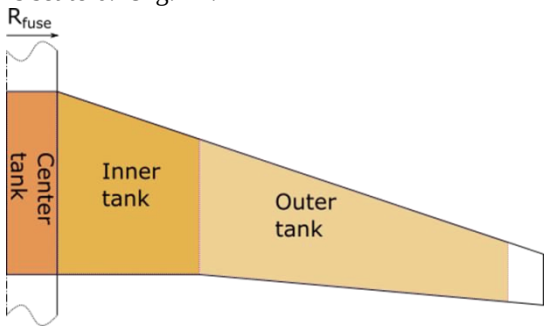

Figure 22- Wing tanks layout.

Finally, the fuel distribution is given by:

$$w_{fuel}(y) = \begin{cases} \rho_{fuel} k_{fill,ct} \left(k_{rear-spar}(y) - k_{front-spar}(y)\right) c_{aero}^2(y) e_{airfoil} & \text{for } y \le R_{fuse} \\ \rho_{fuel} k_{fill,it} \left(k_{rear-spar}(y) - k_{front-spar}(y)\right) c_{aero}^2(y) e_{airfoil} & \text{for } R_{fuse} < y \le y_{kink} \\ \rho_{fuel} k_{fill,ot} \left(k_{rear-spar}(y) - k_{front-spar}(y)\right) c_{aero}^2(y) e_{airfoil} & \text{for } y_{kink} < y \le 0.8 \cdot y_{tip} \end{cases}$$

For simple trapezoidal wings (like most of the upper strutted wings) the inner tank is suppressed ($y_{kink} = R_{fuse}$). The local shear due to fuel is then straightforwardly obtained from:

$$F_{z,fuel}(y_{load}) = \int_{y_{load}}^{b/2} -n_z \cdot g \cdot w_{fuel}(y)dy$$

And the local bending moment is:

$$M_{x,fuel}(y_{load}) = \int_{y_{load}}^{b/2} \frac{F_{z,fuel}(y)}{\cos\phi_e} dy$$

At this stage the torsion due to the fuel is not considered, the underlying hypothesis is that the fuel center of gravity locus is close to the elastic axis.

d. Engine loads

In the new developed model, the loads due to the engine are, to a certain extent, considered. Indeed, only the local shear and bending moment due to the weight are taken into account. While torques resulting from weight and thrust are not computed. The internal engine loads are then given by:

$$F_{z,engine}(y_{load}) = \begin{cases} 0 \; if \; y_{loads} > y_{engine} \\ -n_z \cdot g \cdot W_{engine} \; else \end{cases}$$

$$M_{x,engine}(y_{load}) = \begin{cases} 0 \text{ if } y_{loads} > y_{engine} \\ -n_z \cdot g \cdot W_{engine}(y_{engine} - y_{load}) \text{ else} \end{cases}$$

e. Structural weight loads

The structural weight distribution itself is the source of internal loads. This distribution can be either estimated as elliptic or be computed from the results of the structural sizing. The latter induces a loop between the loads computation and the structure sizing model that is solved in FAST-OAD.

Considering the weight distribution $w_{struct}(y)$, the shear and bending moment are expressed straightforwardly as follows:

$$F_{z,struct}(y_{load}) = \int_{y_{load}}^{\frac{b}{2}} -n_z \cdot g \cdot w_{struct}(y) dy$$

$$M_{x,struct}(y_{load}) = \int_{y_{load}}^{\frac{b}{2}} \frac{F_{z,struct}(y)}{\cos \phi_e} dy$$

f. Strut loads

In the case a strut-braced wing configuration is considered, the loads introduced by the strut within the wing must be accounted for. Because the problem is hyperstatic, the traction in strut in sizing manoeuvre conditions is assumed to represents a portion k_{lift} of the total aircraft lift. It is then hypothesised that the strut could be pre-constrained to reach this force in manoeuvre conditions.

The resulting internal loads are expressed as follows:

$$F_{z,strut}(y_{load}) = \begin{cases} 0 \text{ if } y_{load} > \eta_{strut} \cdot \frac{b}{2} \\ -k_{lift} L \sin \alpha_{strut} \text{ else} \end{cases}$$

$$M_{x,strut}(y_{load}) = \int_{y_{load}}^{b/2} \frac{F_{z,strut}(y)}{\cos \phi_e} dy$$

The normal compressive force introduced in the wing must also be taken into account as it will influence spar flanges sizing as detailed in section 2 and may also be responsible for buckling of the inner wing.

$$F_{y,strut}(y_{load}) = \begin{cases} 0 \text{ if } y_{load} > \eta_{strut} \cdot \frac{b}{2} \\ -k_{lift} L \cos \alpha_{strut} \text{ else} \end{cases}$$

The torque due to the strut is not considered in the current implementation, meaning that the junction with the wing is considered to be located on the elastic axis.

g. Loads envelop

Once all contributions have been computed, the envelop used for the structural sizing can be issued for the

considering load case:

$$F_z(y_{load}) = F_{z,aero}(y_{load}) + F_{z,fuel}(y_{load}) + F_{z,engine}(y_{load}) + F_{z,struct}(y_{load}) + F_{z,\,strut}(y_{load})$$

$$M_x(y_{load}) = M_{x,aero}(y_{load}) + M_{x,fuel}(y_{load}) + M_{x,engine}(y_{load}) + M_{x,struct}(y_{load}) + M_{x,\,strut}(y_{load})$$

$$M_y(y_{load}) = M_{y,aero}(y_{load}) + M_{y,engine}(y_{load}) + M_{y,\,strut}(y_{load})$$

A typical example of internal loads and envelops for a strut-braced wing configuration is provided in Figure 23:

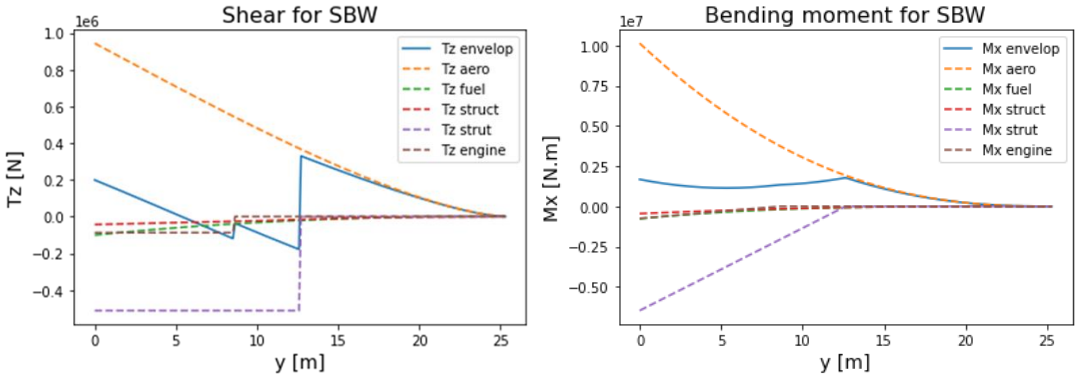

Figure 23- Typical internal loads and envelop for structural sizing for a Strut-braced wing configuration.

2. Analytical wing structure sizing and weight estimate

Once the loads have been properly assessed, the wing primary structure can be sized. The wings and struts primary structure weights are computed using physical analytical models based on beam theory [8], while the weight of the other parts (fuselage, tails, systems, engines, …) are assessed through the semi-empirical formula already implemented in FAST-OAD.

For the new physics-based models developed here, the wing structure is simplified to an equivalent spar plus skin model with the spar flanges supporting bending moment, the web supporting the shear and the skin supporting the torsion (Figure 24).

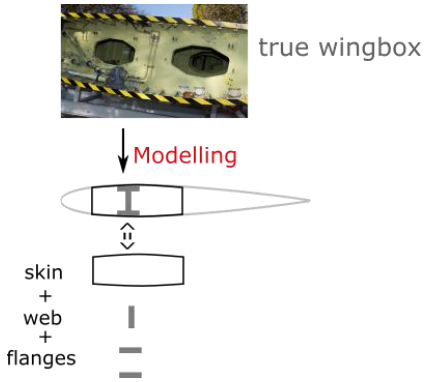

Figure 24- Wing primary structure model for weight computation [8].

This methodology has been extended to the struts considering they only support traction. The models developed here are only valid for isotropic metallic materials. For those materials we consider the tensile yield stress $\sigma_{yield,tens}$, the compressive yield stress $\sigma_{yield,comp}$, the maximum shear stress τ_{max}, the density ρ and a minimum technological thickness for metallic sheets t_{min}, whose typical value is around 2mm.

a. Spar flange sizing

As already mentioned, spar flanges are supposed to support all the bending moment. As a consequence, in the

case of a fully stressed structure and taking into account the minimum technological thickness, the surfaces of the upper and lower flanges are given by:

$$S_{upper-flange}(y) = \max\left(t_{min} \cdot c_{box}(y),\ \left|\frac{-M_x(y)}{h_{spar}(y) \cdot \sigma_{yield,comp}}\right|\right)$$

$$S_{lower-flange}(y) = \max\left(t_{min} \cdot c_{box}(y),\ \left|\frac{M_x(y)}{h_{spar}(y) \cdot \sigma_{yield,tens}}\right|\right)$$

The introduction of a strut implies to consider also the normal compressive force (for positive load factors) acting on flanges:

$$S_{upper-flange}(y) = \max\left(t_{min} \cdot c_{box}(y),\ \left|\frac{-M_x(y)}{h_{spar}(y) \cdot \sigma_{yield,comp}} + \frac{0.5 \cdot T_y(y)}{\sigma_{yield,comp}}\right|\right)$$

$$S_{lower-flange}(y) = \max\left(t_{min} \cdot c_{box}(y),\ \left|\frac{M_x(y)}{h_{spar}(y) \cdot \sigma_{yield,tens}} + \frac{0.5 \cdot T_y(y)}{\sigma_{yield,tens}}\right|\right)$$

The weight of the flanges for both swept wings can be easily derived:

$$W_{flanges} = 2 \cdot \frac{\rho}{\cos\phi_e} \cdot \int_0^{\frac{b}{2}} \left(S_{upper-flange} + S_{lower-flange}\right) dy$$

b. Spar web sizing

The web is supposed to support only the shear. Because expected thicknesses are small enough, the shear flow can be assumed to be constant within the web and the minimal surface allowing a fully stressed structure is given by:

$$S_{web}(y) = \max\left(t_{min} \cdot h_{spar}(y), \frac{F_z(y)}{\tau_{max}}\right)$$

The weight of the web is then obtained straightforwardly:

$$W_{web} = 2 \cdot \frac{\rho}{\cos\phi_e} \cdot \int_0^{\frac{b}{2}} S_{web}\, dy$$

c. Wingbox skin sizing

The torsion shear flow within the wingbox skin is expressed as:

$$\phi(y) = -\frac{M_y(y)}{2S_{box}}$$

Then the minimum allowable thickness for the skins satisfies:

$$t_{skin}(y) \geq \frac{|\phi(y)|}{\tau_{max}} \equiv \left|-\frac{M_y(y)}{2S_{box}(y) \cdot \tau_{max}}\right|$$

With: $S_{box} \equiv S_{ribs} = k_{Sribs} \times e_{airfoil} \times c_{aero}^2 \times \left(k_{rear-spar} - k_{front-spar}\right) \times \cos(\phi_e) \times f_{\phi_e}$

A correction coefficient k_{Sribs} that takes into account the non-rectangular shape of the box in the ribs surface (enclosed by skin) is introduced. Its typical value is around 0.93.

Finally, the local surface of the wingbox skin can be simply derived by the multiplication of skin thickness and wingbox perimeter p.

$$S_{skin}(y) = p(y) \cdot t_{skin}(y)$$

$$\Leftrightarrow S_{skin}(y) = 2 \cdot k_l \cdot \left[e_{airfoil}(y) + \left(k_{rear-spar}(y) - k_{front-spar}(y)\right) f_{\phi_e} \cos\phi_e\right] \cdot c_{aero}(y) \cdot \left|-\frac{M_y(y)}{2S_{box}(y) \cdot \tau_{max}}\right|$$

A correction factor k_l is introduced to take into account the non-rectangular shape of the box in the computation of perimeter. A typical value for this coefficient is 0.97.

d. Strut sizing

The strut is assumed to support only traction force (compression case is eluded at this stage of development). The chord of the strut being considered as constant, the surface to sustain loads is given by:

$$S_{strut} = \max\left(t_{min} \cdot 2 \cdot \left(c_{box,strut} + h_{box,strut}\right),\ \frac{k_{lift} \cdot L}{\sigma_{yield,tens}}\right)$$

And the weight for both side struts is directly derived from the length l_{strut} of a strut:

$$W_{strut} = 2 \cdot \rho \cdot S_{strut} \cdot l_{strut}$$

e. Total wing weight

Finally, the total wing weight is computed adding the contribution of skin, flanges and web and considering also ribs and secondary parts through empirical formulations. The ribs are supposed to be evenly spaced spanwise with a constant thickness fixed by the user. The secondary structure is computed with the following formula:

$$W_{wing,sec} = 0{,}3285 \cdot k_{wing} \cdot MTOW^{0{,}35} \cdot S_{cantilever} \cdot k_{mvo}$$

With k_{wing} and k_{mvo} that are respectively a correction coefficient depending on engine layout (its value is 1 for 4 engine aircraft, 1.05 for two engines and 1.1 for rear engines) and a "cultural" coefficient to take into account structural additional weights. $S_{cantilever}$ is the cantilevered surface of the wing (outside fuselage).

3. Verification of the analytical SBW structural weight model

As a verification of the response of the SBW structural weight estimation model, parametric studies of the response of the model to different parameters such as the aspect ratio of the wing, the spanwise location of the strut junction on the wing, strut traction load and wing box thickness have been conducted. These exercises were conducted for a total aerodynamic loading on the wing assumed to be constant and elliptically distributed along the span.

The impact of the spanwise location of the strut on the wing and of the traction force in the strut (expressed as a fraction of the total wing aerodynamic load, L) is illustrated in Figure 25 for a wing of aspect ratio fixed at 16. This clearly shows, for each strut traction value, an optimum strut attachment location and the global optimum of this parameter being around 65% of the span, from a pure structural weight perspective.

The investigation of the effect of the aspect ratio on the minimal structural wing+strut weight for the SBW is illustrated in Figure 26 (orange line in the bottom left plot). This figure also shows the weight of a cantilever wing structure, sized with the same approach and hypothesis, for different aspect ratios. The potential of the SBW to alleviate the structural wing weight increase with AR is clearly demonstrated by a much slower increase of the wing weight with aspect ratio for the SBW. In these last results, the wing weight was minimised by identifying the optimal value of strut junction location and strut traction. The bottom right plot of Figure 26 shows the evolution of the optimal values of these two parameters with aspect ratio.

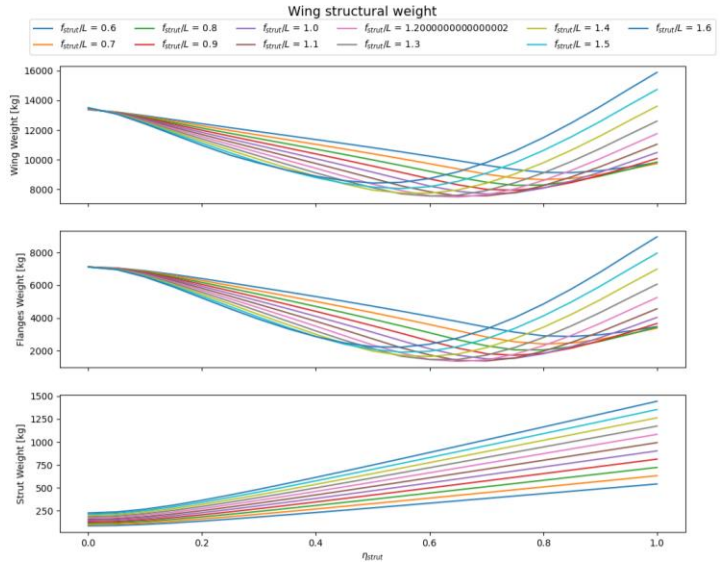

Figure 25- Investigation of the impact of spanwise strut/wing junction location on the primary wing (flange), strut and total wing+strut weights

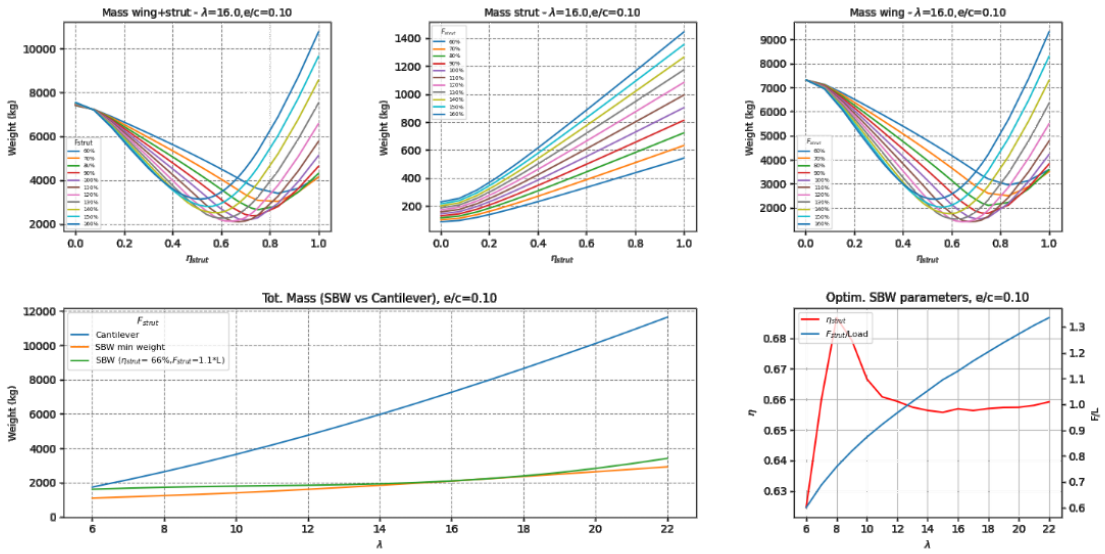

Figure 26- Investigation of the impact of the AR of the wing on the optimal SBW wing+strut structural weight. For each value of the AR, the spanwise location of the strut attachment and the internal strut traction loading is optimized to achieve minimum weight

B. High fidelity structural analyses

The high-fidelity structural model used to develop the design methodology is the FEM model of the ALBATROS project illustrated in Figure 27. The particularity of this model is to use a curved strut in order to mitigate buckling problems. Static computations of this strut braced wing configuration have been made using the FEM code MSC Nastran in linear and non linear approaches (see Figure 28 and Figure 29). Taking the aerodynamic forces into account in these computations will be the next step of this work.

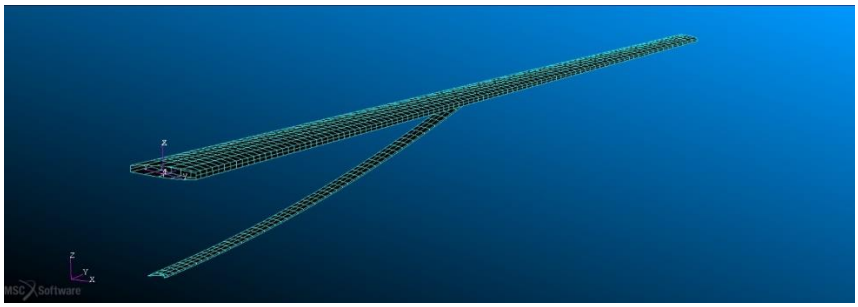

Figure 27– Finite Element Model of ALABATROS strut braced wing

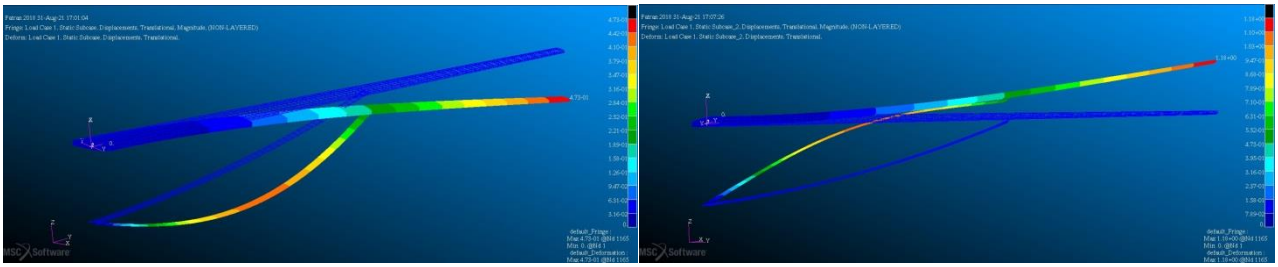

Figure 28- Linear computation with MSC Nastran of static deflection in two sizing cases (-1.g on the left and +2.5g on the right)

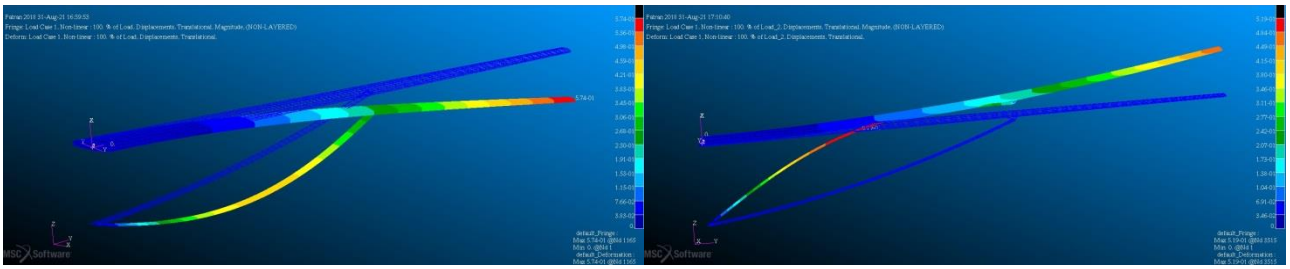

Figure 29- Nonlinear computation with MSC Nastran of static deflection in two sizing cases (-1.g on the left and +2.5g on the right)

VI. Results of the OAD process applied to investigate the potential benefits of HAR-SBW concept

A. Aircraft designs evaluations using FAST-OAD process

One of the main interests of the FAST-OAD process lies in the ability to quickly evaluate different aircraft designs. This opportunity is particularly given by the possibility to implement custom modules to evaluate the performances of unconventional configurations. To illustrate this feature, the reconstruction of a cantilever equivalent of the reference SBW configuration starting from the A321-LR configuration is detailed in the following.

Starting from the reconstruction of the A321-LR, the first modification, motivated both by the aerodynamics and the structural disciplines, consisted in moving the engines from their position under the wing to a rear position on the fuselage. In the same time, the geometry of the tail is modified from a conventional tail to a T-Tail geometry, preserving the effectiveness of the HTP. These modifications are shown in Figure 30.

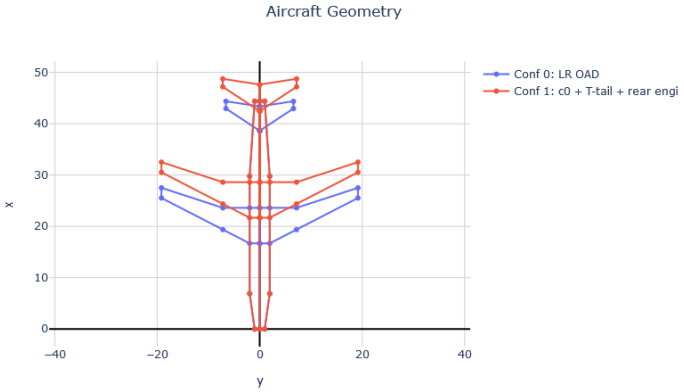

Figure 30 - Geometry modifications modelled by FAST-OAD after rear positioning of the engines

Additional geometry modifications lead to the reproduction of the SBW reference configuration ALBATROS, illustrated in green in Figure 31.

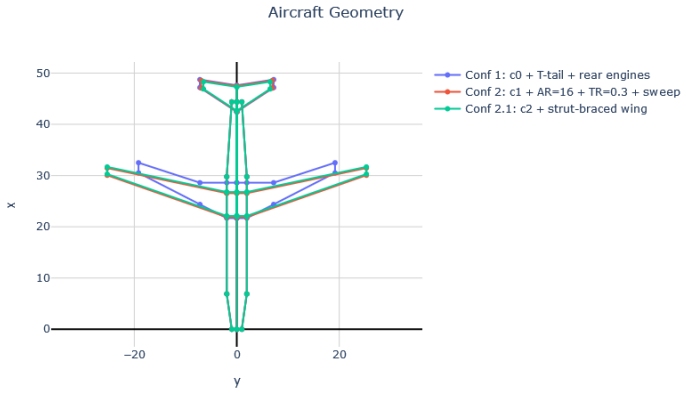

Figure 31 – Reproduction of the ALBATROS SBW configuration with FAST-OAD

As illustrated in Figure 31, the wing geometry is changed between conf 1 (in blue) and conf 2 (in red) by modelling a simple trapezoidal wing with an aspect ratio $AR = 16$. The sweep angle of the configuration is also reduced to match the sweep angle of the ALBATROS configuration, which is supposed to extend the laminar portion of the wing. Finally, a generic strut is added to this last configuration in the configuration 2.1 (in green). The mass breakdown of these configurations is presented in Figure 32.

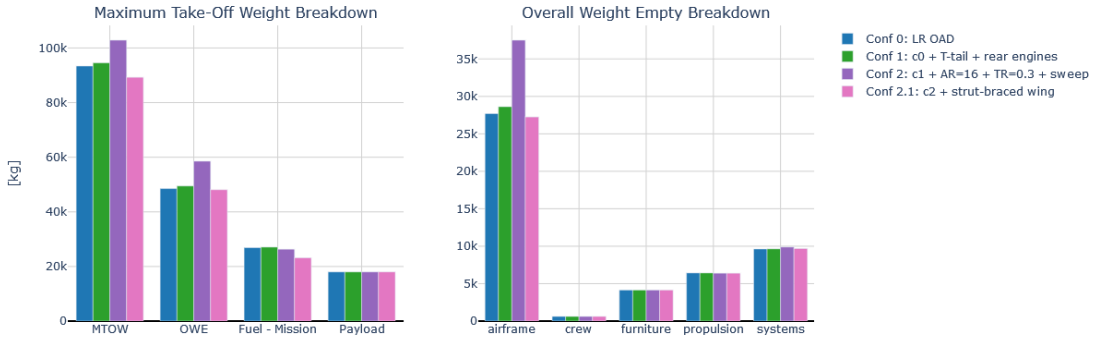

Figure 32 - Mass breakdown comparison for the reproduced ALBATROS configuration

The interest of the FAST-OAD process resides in the possibility to quickly evaluate and compare cantilever and SBW configurations. From this preliminary analysis, the strut would allow reducing the fuel needed by about 12% to achieve the Breguet-Leduc mission that was defined.

B. Fast evaluation of the aspect ratio influence on the SBW configuration using FAST-OAD

From the positive results of the previous paragraph, next step consists in starting to optimize the SBW configuration by sweeping over the AR parameter.

Several geometries of the SBW configuration are then considered, starting from the swept configuration with an AR = 16 introduced in part A of this section. The FAST-OAD analysis is performed for the aspect ratios $AR \in [10, 12, 14, 16, 20, 22]$ in combination with the position of the junction between the strut and the wing written $\eta_{strut} = \frac{y_{junction}}{b}$. For this analysis, the Breguet-Leduc equation is considered to determine the fuel weight needed by the aircraft to achieve the mission.

The fixed main geometrical parameters of the SBW configuration are the strut wetted surface and the aspect ratio while the variables of interest are the wing span and the wing planform area. The main quantities of interest determined in the end by the FAST-OAD process are the MTOW, block fuel and wing mass, which are expected to decreased if compared with a classical cantilever configuration. The evolutions of these quantities are illustrated in the following figures, where the values plotted for $\eta_{strut} = 0$ corresponds to the cantilever configuration of the airplane:

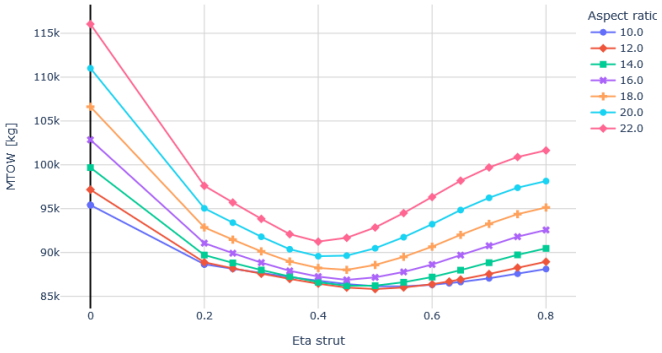

a) Influence of the position of the junction on the MTOW

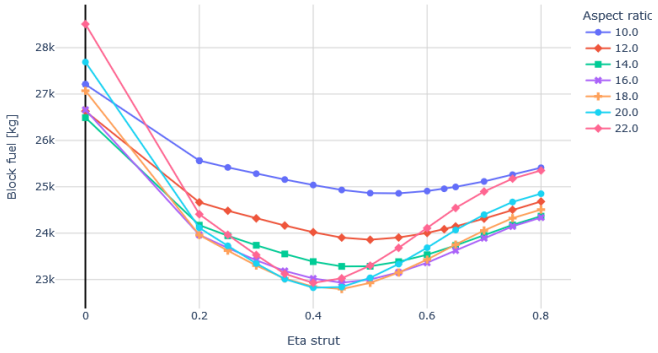

b) Influence of the position of the junction on the block fuel mass

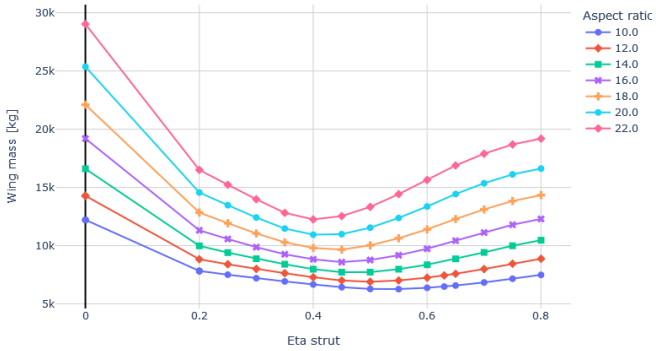

c) Influence of the position of the junction of the wing mass

Figure 33 - Preliminary study of the influence of the Aspect Ratio of the SBW configuration

As can be seen from Figure 33, the presence of a strut presents a direct advantage compared to a cantilever configuration from a mass reduction perspective, and this for all the aspect ratio considered. From these images, it seems that an optimum position for the junction between the strut and the wing is appearing between 40% and 50% of the wingspan, depending on the aspect ratio. This particularity will be more precisely studied in the future.

VII.Conclusion and Perspectives

In the context of the EU funded Clean-Sky 2 project U-HARWARD [6], a multi-fidelity investigation of the SBW configuration has been initiated in 2020 by ONERA and ISAE-SUPAERO. A multi-disciplinary and multi-level design approach has been set up combining an overall aircraft conceptual design framework, FAST-OAD[7] and high-fidelity disciplinary analysis and design frameworks for aerodynamics and structures. The logic of this multi-level approach is to feed the conceptual design process with physics-based information from high-fidelity analyses and design tasks from the aerodynamics and structural disciplines.

The disciplinary models initially embedded in the FAST-OAD conceptual design framework were based on empirical and semi-analytical formulas that provide a consistent response to overall aircraft parameters for conventional tube-and-wing aircraft configurations. To investigate SBW configurations, these FAST-OAD legacy models have been complemented or substituted by an analytical structural sizing model for what concerns wing weight estimation and a strut drag penalty model derived from high-fidelity CFD simulations of SBW configurations.

The OAD process embedding these new models for the wing structure and aerodynamic specifically developed for SBW configuration has been applied to perform first investigations of the SBW concept. Although the first results of these OAD investigations include some conservative hypotheses and therefore do not yet take full benefits of the SBW concept (e.g. wing airfoil thickness reduction and natural laminar flow potential on the wing are not accounted for at this stage), the potential benefits of a HAR-SBW aircraft configuration aircraft are clearly identified, compared to a conventional tube-and cantilever-wing aircraft designed for the same mission corresponding to the one of a Airbus A321-LR. A parametric investigation of the effect of the wing aspect ratio showed an optimum benefit in term of block-fuel reduction for a value of the aspect ratio around 20. For such high aspect ratio values, thanks to the strut, the OEW is even reduced compared to a conventional tube-and-wing aircraft thanks to the snowball effects and therefore the MTOW is significantly reduced.

This SBW concept investigation will be consolidated and further elaborated in the future, with the exploration of additional wing design parameters such as the wing thickness distribution, or by accounting for the potential drag reduction benefits achievable by natural laminar flow on the low sweep, thin wing enabled by the SBW concept.

VIII. Acknowledgment

The work presented in this paper has been funded by the European Union in H2020-EU.3.4.5.10 through the CleanSky2 project U-HARWARD, under grant Grant agreement ID: 886552

IX. References

[1] https://op.europa.eu/fr/publication-detail/-/publication/296a9bd7-fef9-4ae8-82c4-a21ff48be673
[2] Fayette Collier, Status of Research and Development of the Hybrid Wing Body (HWB) Aircraft Concept, 7th UTIAS International Workshop on Aviation and Climate Change, May 2021, Toronto
[3] M. Iwanizki, S. Wöhler, B. Fröhler, T. Zill, M. Méheut, S. Defoort, M. Carini, J. Gauvrit-Ledogar, R. Liaboeuf, A. Tremolet, B. Paluch, S. Kanellopoulos, Conceptual Design Studies Of Unconventional Configurations, 3AF Aerospace Europe Conference 2020, Feb2020, BORDEAUX, France. hal-02907205
[4] Zhenli CHEN, Minghui ZHAN, Yingchun CHEN, Weimin SAN, Zhaoguang TAN, Dong LI, Binqian ZHANG Assessment on Critical Technologies for Conceptual Design of Blended Wing Body Civil Aircraft. Chinese Journal of Aeronautics, 2019, 32(8): 1797-1827
[5] G. Carrier, O. Atinault, S. Dequand, J.-L. Hantrais-Gervois, C. Liauzun, B. Paluch, A.-M. Rodde, C. Toussaint, Investigation of a strut-braced wing configuration for future commercial transport, ICAS, 28th congress of the aeronautical sciences, 23-28 September 2012, Brisbane, paper 597.
[6] https://www.u-harward-project.eu/, last accessed Nov 2021.
[7] Christophe David Christophe David, Scott Delbecq, Sébastien Defoort, PeterSchmollgruber, Emmanuel Benard, Valérie Pommier-Budinger, From FAST to FAST-OAD: An open source framework for rapid Overall Aircraft Design, 2021 IOP Conf. Ser.: Mater. Sci. Eng.1024 012062.
[8] https://ceras.ilr.rwth-aachen.de/tiki/tiki-index.php?page=CSR-01&structure=CeRAS
[9] Roux, E. “Pour une approche analytique de la dynamique du vol”, PhD Thesis, Univ. Toulouse, 2005
[10] Drela, M. and Youngren, H., http://web.mit.edu/drela/Public/web/avl/

[11] R. Haimes and J. F. Dannenhoffer, “The Engineering Sketch Pad: A Solid-Modeling, Feature-Based, Web-Enabled System for Building Parametric Geometry,” in 21st AIAA Computational Fluid Dynamics Conference, 2013.
[12] Michael A. Park, William L. Kleb, William T. Jones, Joshua A. Krakos, Todd R. Michal, Adrien Loseille, Robert Haimes and John Dannenhoffer, “Geometry Modeling for Unstructured Mesh Adaptation”, AIAA Paper 2019-2946, https://doi.org/10.2514/6.2019-2946
[13] Christopher M. Meckstroth, “Parameterized, Multi-fidelity Aircraft Geometry and Analysis for MDAO Studies using CAPS”, AIAA Paper 10.2514/6.2019-2230
[14] Destarac, D., and van der Vooren, J.,
“Drag/Thrust Analysis of Jet-Propelled Transonic Transport Aircraft: Definition of Physical DragComponents,” Aerospace Science and Technology, Vol. 8, No. 6, 2004,pp. 545–556
[15] Raymer D.P., “Aircaft design : a conceptual approach”, AIAA Education Series, 5th edition, Sep 2012.
[16] Steve Karman, Nick Wyman, “Automatic Unstructured Mesh Generation with Geometry Attribution”, AIAA Paper 10.2514/6.2019-1721
[17] “OpenCASCADE.” [Online]. Available: https://www.opencascade.com/.
[18] G. Carrier, C. Blondeau, F. Moens, M. Carini, Thomas Le Garrec and Daniel Mincu, “Illustrations of multi-disciplinary high-fidelity analysis capabilities for aero-structural and aero-acoustic aircraft design”, AIAA Paper 2021-1316 presented at AIAA Scitech 2021 Forum, 11–15 & 19–21 January 2021. https://doi.org/10.2514/6.2021-1316
[19] B. Kulfan, “A Universal Parametric Geometry Representation Method – CST”, AIAA Paper 2007-0062
[20] GN. Vanderplaats, “A robust Feasible Directions algorithm for design synthesis”. AIAA Paper 83-0938, 24th Structures, Structural Dynamics and Materials Conference, Lake Tahoe, NV, 1983.
[21] Palacios, F., Colonno, M. R., Aranake, A. C., Campos, A., Copeland, S. R., Economon, T. D., Lonkar, A. K., Lukaczyk, T. W., Taylor, T. W. R., and Alonso, J. J., *“Stanford University Unstructured (SU2): An Open-source Integrated Computational, Environment for Multi-Physics Simulation and Design"*, 51st AIAA Aerospace Sciences Meeting, Grapevine, Texas, 2013
[22] Andy Ko, William Mason and Bernard Grossman. *"Transonic Aerodynamics of a Wing/Pylon/Strut Juncture"* AIAA 2003-4062. 21st AIAA Applied Aerodynamics Conference. June 2003